25·29 August 2024
inter.noise
NANTES FRANCE

A vibroacoustic model for low-frequency sound transmission loss in circular membranes with added strip mass.

Ajju Raja Justus[1]
Department of Mechanical Engineering,
Indian Institute of Technology Palakkad, Kerala, India -678623

Anoop Akkoorath Mana[2]
Department of Mechanical Engineering,
Indian Institute of Technology Palakkad, Kerala, India -678623

ABSTRACT

Noise control strategies involve physical barriers in the transmission path. Conventional barriers conform to the mass law which states an inverse relation between sound transmission, barrier mass, and incident frequency. Practical scenarios for low-frequency noise attenuation require prohibitively thick barriers making them infeasible. Mass-loaded membranes exhibit marked differences in their dynamic nature from that of bare membranes as they do not necessarily conform to the mass law. Being thin, compact, and lightweight makes them geometrically ideal for most applications. The paper presents an analytical model based on the Newtonian approach for the vibroacoustic behavior of a pre-stretched elastic circular membrane with rigidly attached strip mass under normal incidence. The point collocation approach distributes the effect of the strip mass on the membrane as a collection of discretized concentrated loads along the interfacial boundary resulting in a summation that is easier to solve. The peak and dip frequencies of sound transmission are determined for circular membranes with eccentric and central strip mass. The present study evaluates strip mass-loaded membranes' capability to attenuate noise at low frequencies as an unconventional physical barrier.

1. INTRODUCTION

Increasing use of mass-loaded membranes in space, energy harvesting, sound transducer, and noise attenuation applications [1–4] are encouraging researchers to more accurately study and manipulate the membrane's dynamic nature as per the requirements of the application. Added masses alter the vibrational behavior of a membrane by increasing its potential energy. Simplified studies on membranes with finite masses began as early as [5, 6]. The studies [7–9] helped Chen et.al [10] develop a vibroacoustic model for circular membranes with finite rigid disc mass to analyze its sound transmission characteristics. The effect of the mass on the membrane is considered using the point collocation method [11] wherein the weight of the mass is distributed as a summation of point loads at discrete circumferential locations. The approach considers the

[1]132204001@smail.iitpkd.ac.in
[2]akkoorath@iitpkd.ac.in

continuity of displacement at collocation points along the interfacial mass-membrane boundary and solves the homogeneous system to understand the modal behavior.

The present work extends the existing theoretical model based on the Newtonian approach to strip mass. The point collocation method accurately captures the rigid body motion of the strip mass and its effect on the stretched elastic membrane. The eigenvalue analysis determines the mode shapes and resonance of the system. The incident acoustic wave excites the membrane and causes sound radiation. This effect is considered in the governing equation to understand the membrane's vibroacoustic behavior. The modal superposition approach solves the vibroacoustic integrodifferential equation for the membrane displacement field. The peak and dip frequencies help determine the sound transmission characteristics of the mass-loaded membrane in the low-frequency range. This study underlines the effect of strip mass on a circular membrane's low-frequency sound transmission characteristics. It is hoped that the results will help further the utility of strip masses in low-frequency noise control.

2. EIGENVALUE PROBLEM

Consider a circular membrane (see Figure 1) of radius R, surface density ρ_s and pre-tension T fixed at the outer periphery. A strip mass of width V, and surface density ρ_m are rigidly attached to the membrane at an eccentricity d from the membrane center. Global polar coordinate system (r,θ) with membrane center at origin O and local polar coordinate system (r',θ') with mass center at origin O' define the membrane model.

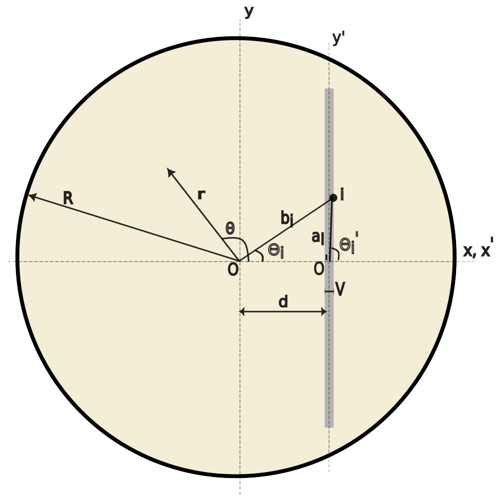

Figure 1: Circular membrane with eccentric strip mass

The governing equation for the membrane (Equation 1) in polar coordinates is,

$$\rho_s\, w_{,tt} - T(w_{,rr} + \frac{1}{r} w_{,r} + \frac{1}{r^2} w_{,\theta\theta}) = \sum_{i=1}^{I} Q_i(t)\, \frac{1}{r}\, \delta(r-b_i)\, \delta(\theta-\Theta_i), \tag{1}$$

where the effect of the strip mass weight on the membrane is considered as a summation of discrete point forces Q_i distributed over the interfacial boundary between the mass and the membrane. δ is the unit impulse function. The study considers steady-state response and suppresses $e^{j\omega t}$ for all the terms. Equation 2 is the restructured form of Equation 1,

$$\alpha^2\, w + (w_{,rr} + \frac{1}{r} w_{,r} + \frac{1}{r^2} w_{,\theta\theta}) = -\sum_{i=1}^{I} \left[N_i\, \frac{b_i}{r}\, \delta(r-b_i)\delta(\theta-\Theta_i) \right], \tag{2}$$

where $\alpha = \rho_s\omega^2/T$, ω is the angular frequency, $N_i = Q_i/(b_i T)$, b_i is the radial coordinate of the i^{th} collocation point from O. The general solution (Equation 3) is a linear combination of the homogeneous solution (variable separation) and the particular solution (Lagrange's method of variation of parameters).

$$w(r,\theta) = +\sum_{n=0}^{\infty} \epsilon_n \Big\{ A_{1n} J_n(\alpha r) - \frac{1}{2}\sum_{i=1}^{I} N_i b_i \left[Y_n(\alpha r) J_n(\alpha b_i) - J_n(\alpha r) Y_n(\alpha b_i) \right] u(r-b_i) \cos n\Theta_i \Big\} \cos n\theta$$
$$+\sum_{n=0}^{\infty} \epsilon_n \Big\{ A_{2n} J_n(\alpha r) - \frac{1}{2}\sum_{i=1}^{I} N_i b_i \left[Y_n(\alpha r) J_n(\alpha b_i) - J_n(\alpha r) Y_n(\alpha b_i) \right] u(r-b_i) \sin n\Theta_i \Big\} \sin n\theta, \tag{3}$$

where $J_n(\alpha r), Y_n(\alpha r)$ are the first and second kind Bessel functions of order n. ϵ is a constant with values 0.5 and 1 when n = 0 and n > 0 respectively. A_{1n}, A_{2n} are unknown constants for symmetric and antisymmetric modes (about the axis of symmetry), determined from the condition of fixed membrane outer boundary, $w(R,\theta) = 0$. N_i and N_i^* are the unknown constants for the point loading at the i^{th} collocation point for symmetric and antisymmetric modes respectively. The condition of mass-membrane displacement continuity at the collocation points, $w(r,\theta) - w'(a,\theta') = 0$ results in an eigenvalue problem. Solving for the roots of this characteristic equation gives the eigenfrequencies and subsequently the corresponding unknown constants N_i and N_i^*. Back substituting the values into Equation 3 gives the mode shapes of the mass-loaded membrane.

2.1. Results and Discussion

The present study considers circular membranes with a central strip mass and strip mass with an eccentricity of 4mm and 6mm. The analytical model helps understand the effect of mass position on the membrane eigenmodes. The relevant properties are provided in Table 1. The membrane's three lowest natural frequencies (Table 2) and modeshapes (see Figure 2) for symmetric modes demonstrate the effect of the mass position on the eigenmodes. The black line in the plots (see Figure 2) represents the reference configuration of the strip mass. The lowest natural frequency increases with an increase in eccentricity while the other two natural frequencies decrease with an increase in eccentricity.

Table 1: Mass and membrane parameters.

	Membrane	**Mass**
Mass density (kg/m^3)	980	8960
Young's modulus (Pa)	2 x 10^5	130 x 10^9
Poisson ratio	0.49	0.34
Weight (kg)	-	40.32 x 10^{-6}
Pretension (T)	51.2	-
Radius (m)	0.01	-
Width (m)	-	0.0001

For the central strip mass, the strip mass's translatory motion contributes to the membrane's large amplitude transverse displacement and is characterized as the first eigenmode. The second and the third eigenmodes have increased contribution from the membrane motion and lesser

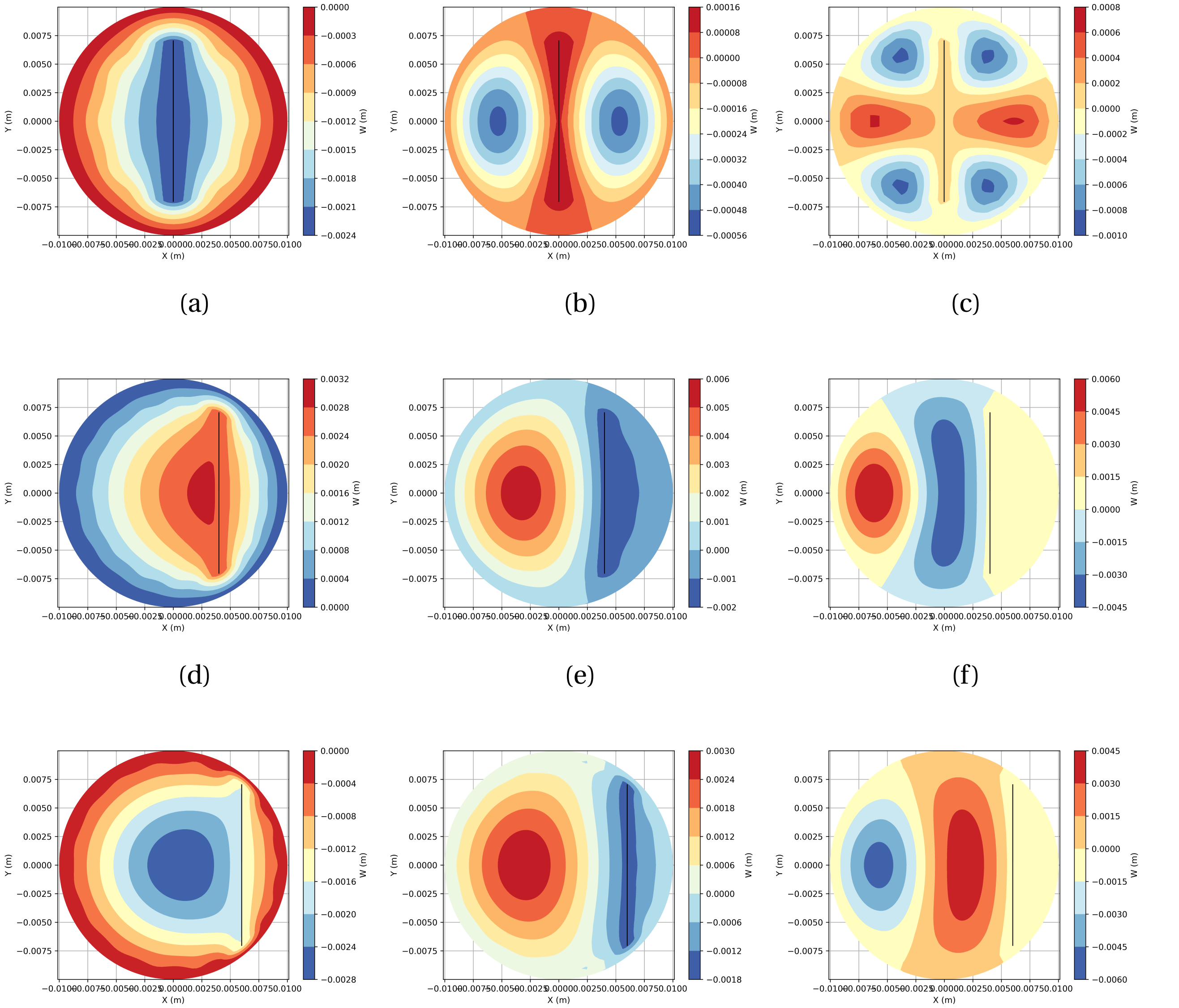

(a) (b) (c)

(d) (e) (f)

(g) (h) (i)

Figure 2: First three symmetric modes of the circular membrane with zero eccentricity (a-c), 4mm eccentricity (d-f), and 6mm eccentricity(g-i).

Table 2: Lowest three eigenfrequencies of the strip mass at different eccentricity

	First (Hz)	**Second (Hz)**	**Third (Hz)**
Concentric mass (d = 0mm)	383.4	923.9	1440.5
Eccentric mass (d = +4mm)	413.7	683.8	1103.7
Eccentric mass (d = +6mm)	493.2	661.6	999.3

contribution from the strip mass. For the eccentric strip mass, the eccentricity introduces rotational effects that modify the eigenmodes.

3. VIBROACOUSTIC MODEL

Consider a plane wave $\tilde{p}_I$ (equal to $\tilde{P}_I e^{-jk_a z}$) incident on the circular membrane placed in a cylindrical tube. k_a is the wave number of the acoustic medium (air). The membrane set into motion by the incident wave causes pressure variations in the medium, resulting in sound radiation. Equation 4 captures the membrane's fully coupled vibroacoustic behavior by considering the acoustic loading in addition to pretension and the external mass,

$$\rho_s w_{,tt} - T(w_{,rr} + \frac{1}{r} w_{,r} + \frac{1}{r^2} w_{,\theta\theta}) = \tilde{p}_1\big|_{z=0} - \tilde{p}_2\big|_{z=0} + \sum_{i=1}^{I} Q_i(t)\, \frac{1}{r}\, \delta(r-b_i)\, \delta(\theta - \Theta_i), \tag{4}$$

where $\tilde{p}_1$, $\tilde{p}_2$ are the pressure fields to the left and right of the interface. The thickness effects of the membrane are neglected. Conditions of steady-state response, geometric symmetry, divergence of Y_n at the membrane center, and rigid side wall ($\frac{\partial \tilde{p}}{\partial r}\big|_{r=R} = 0$) applied to the linear acoustic wave equation provides the pressure field of the excited membrane that contains both $\tilde{p}_1$, $\tilde{p}_2$. Superposition with the incident acoustic wave gives the total pressure field of the membrane (Equation 5),

$$\tilde{p}_{total}(r,\theta,z) = \tilde{P}_I e^{-jk_a z} + \sum_{m=0}^{\infty}\sum_{l=0}^{\infty} \tilde{A}_{ml} J_m(k_r^{ml} r)\cos(m\theta) e^{jk_z^{ml} z} + \sum_{m=0}^{\infty}\sum_{l=0}^{\infty} \tilde{B}_{ml} J_m(k_r^{ml} r)\cos(m\theta) e^{-jk_z^{ml} z}, \tag{5}$$

where *'m'* and *'l'* represent the considered order and points of zero crossing of the Bessel function respectively. Sorting Equation 5 into pressure fields to the left and right of the interface helps determine the acoustic loading (see Figure 3 and Equation 6),

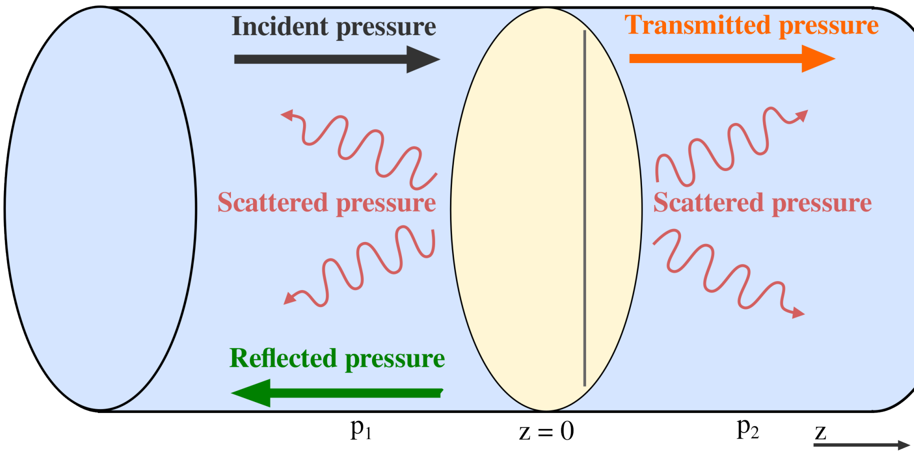

Figure 3: Strip mass loaded membrane subjected to acoustic loading in a cylinder.

$$\begin{aligned} \tilde{p}_1(r,\theta,0) &= \tilde{P}_I + \tilde{P}_R + p^{-}{}_{|z=0} \\ \tilde{p}_2(r,\theta,0) &= \tilde{P}_T + p^{+}{}_{|z=0}, \end{aligned} \tag{6}$$

where $\tilde{P}_I$, $\tilde{P}_R$, $\tilde{P}_T$ are the plane incident, reflected and transmitted pressure fields respectively and p^-, p^+ are the higher order scattered pressure field. At the interface (z=0) between the membrane and the acoustic medium, the membrane vibrates in phase with the medium. This and the linearized Euler's equation collectively relate the acoustic pressure with the membrane displacement. The membrane displacement is also resolved into average displacement field <w> that relates to the plane waves and the δw that relates to the higher order scattered waves (Equation 7),

$$\frac{\partial p_1}{\partial z}\bigg|_{z=0} = \frac{\partial p_2}{\partial z}\bigg|_{z=0} = \omega^2 \rho_a (< w > + \delta w). \tag{7}$$

The solution provides the following relations,

$$\tilde{P_T} = j\omega\rho_a c_a < w >, \tag{8}$$

$$\tilde{P_R} = \tilde{P_I} - \tilde{P_T}, \tag{9}$$

$$\begin{aligned} \tilde{p}^-\big|_{z=0} &= -\tilde{p}^+\big|_{z=0} \\ &= \tilde{P}(r,\theta,0). \end{aligned} \tag{10}$$

Acoustic loading is the difference between $\tilde{p}_1$, $\tilde{p}_2$,

$$\tilde{p}_1 - \tilde{p}_2 = \tilde{P_I} + \tilde{P_R} + p^-{}_{|z=0} - (\tilde{P_T} + p^+{}_{|z=0}). \tag{11}$$

Substituting Equation 9 and Equation 10 into Equation 11 gives the compact expression for the acoustic loading,

$$\tilde{p}_1 - \tilde{p}_2 = 2(P_I - P_T + \tilde{P}(r,\theta,0)). \tag{12}$$

Green's function coupled with Gauss divergence theorem provides the system response to the scattered field by understanding the system response to an impulsive force (Dirac delta),

$$\begin{aligned} P(r,\theta,0) &= \int_{-\pi}^{\pi}\int_0^R G(r,\theta,0,r^*,\theta^*,0)\,\frac{\partial P(r^*,\theta^*,z^*)}{\partial z^*}|_{z^*=0}\, r^* dr^* d\theta^* \\ &= \omega^2\rho_a \int_{-\pi}^{\pi}\int_{-0}^{R} G\delta w r^* dr^* d\theta^*. \end{aligned} \tag{13}$$

The Green's function G for the domain is,

$$G = \frac{e^{jk_aS}}{4\pi S} + \frac{e^{jk_aS_1}}{4\pi S_1},$$

with the boundary condition being,

$$\frac{\partial G}{\partial z}|_{z=0} = 0, \tag{14}$$

and

$$\begin{aligned} S &= \sqrt{r^2 + r^{*2} - 2rr^*\cos(\theta-\theta^*) + (z-z^*)^2}, \\ S_1 &= \sqrt{r^2 + r^{*2} - 2rr^*\cos(\theta-\theta^*) + (z+z^*)^2}, \end{aligned} \tag{15}$$

where S and S_1 represent the distance between the source and field points to the left and right of the interface respectively. Equation 16 is the governing equation of the fully-coupled vibroacoustic model obtained by combining Equations 4, 8, 12 and 13.

$$-\rho_s\omega^2 \mathrm{w} - T\nabla^2\mathrm{w} + 2i\omega\rho_a c_a < \mathrm{w} > -2\omega^2\rho_a\int_{-\pi}^{\pi}\int_0^R G\delta \mathrm{w} r^* dr^* d\theta^* = 2P_I + \sum_{i=1}^{I} Q_i \frac{1}{r}\delta(r-b_i)\delta(\theta-\Theta_i), \tag{16}$$

where < w > represents the average displacement (that relates to plane waves) and 'δw' is the displacement field that relates to the higher order scattered wave field. To solve the integrodifferential equation, the mode superposition approach is utilized wherein the membrane displacement is considered as a summation of displacement modes,

$$\mathrm{w} = \sum_{k=1}^{+\infty} W_k(r,\theta) q_k, \tag{17}$$

where W_k is the k^{th} mode displacement function and q_k is the unknown participation factor of the k^{th} displacement mode. The mathematical expression for $W_k(r,\theta)$ is as given in Equation 3,

$$(\omega_l^2-\omega^2)(\rho_s\pi R^2 < W_l^2 > +m\overline{c}_l^2 + I_y^{'}\overline{a}_l^2 + I_x^{'}\overline{b}_l^{2})q_l + \sum_{k=1}^{+\infty} 2i\omega\rho_a c_a\pi R^2 < W_l >< W_k > q_k \\ -\sum_{k=1}^{+\infty} 2\omega^2\rho_a \left[\int_{-\pi}^{\pi}\int_0^R W_l \int_{-\pi}^{\pi}\int_0^R G(W_k - < W_k >)\, r^* dr^* d\theta^*\right] q_k = 2P_I\pi R^2 < W_l >, \quad (18)$$

where a_l,b_l,c_l,d_l are the constants for the rigid body motion of the strip mass for the l^{th} displacement mode. The constant q_k is obtained by solving the above system of equations. The sound transmission coefficient is,

$$\tilde{T} = \frac{P_T}{P_I} = \frac{j\omega\rho_a c_a < w >}{P_I}, \quad (19)$$

where $< w >= \sum_{k=1}^{+\infty} < W_k(r,\theta) > q_k$ based on mode superposition method and the transmission intensity coefficient T_I is $|\tilde{T}^2|$.

3.1. Results and Discussion

The sound transmission characteristics of the strip mass-loaded membrane with a central strip mass (see Figure 4) show transmission peaks at around 350 Hz and 900 Hz and dips at around 700 Hz and 1400 Hz. The maximum sound transmission loss occurs at around 700 Hz.

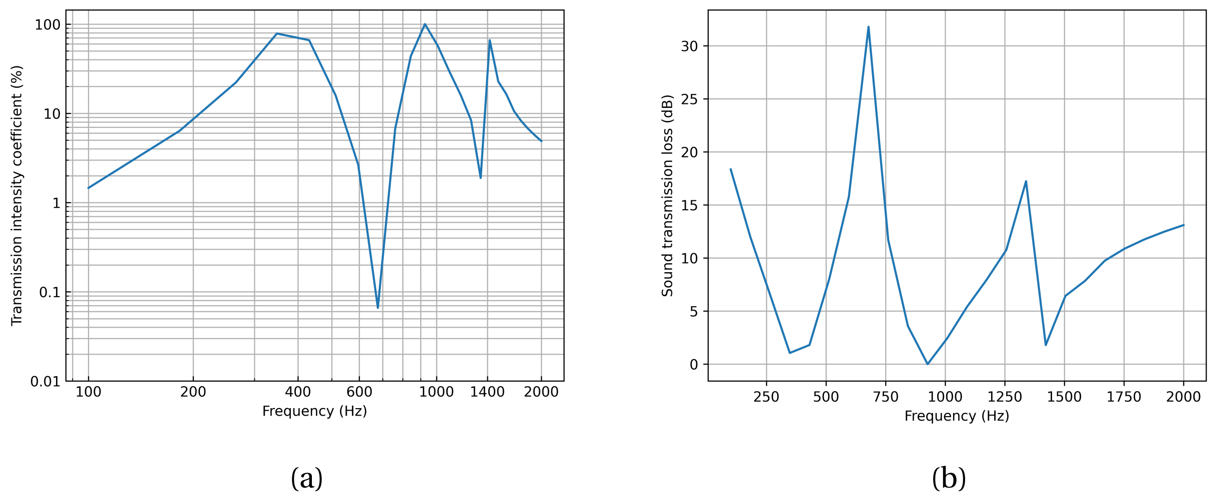

Figure 4: Circular membrane with central mass: (a) represents the transmission intensity coefficient. (b) represents the sound transmission loss.

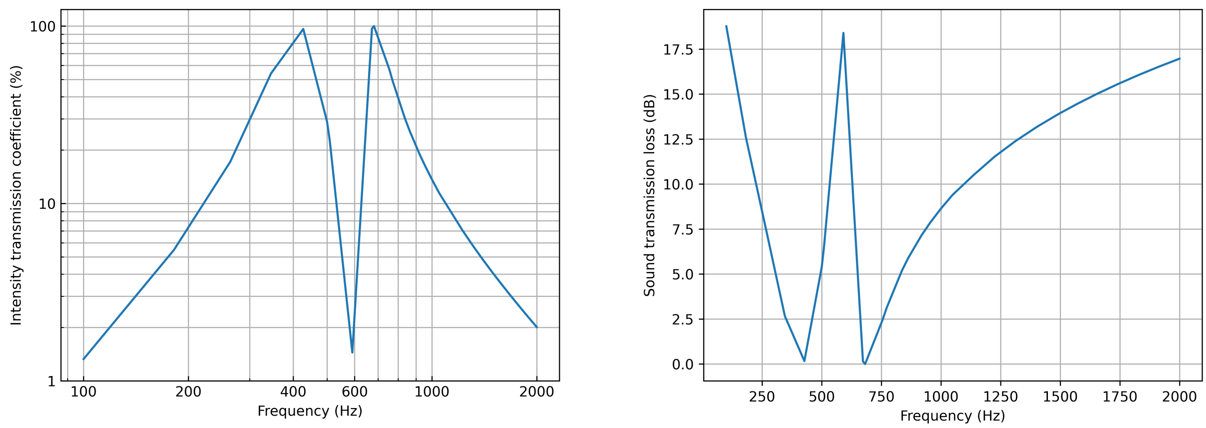

(a) (b)

Figure 5: Circular membrane with eccentric mass (d = 4mm): (a) represents the transmission intensity coefficient. (b) represents the sound transmission loss.

The sound transmission characteristics of the strip mass-loaded membrane with an eccentric strip mass (see Figure 5) show transmission peaks at around 400 Hz and 700 Hz and dips at around 600 Hz. The maximum sound transmission loss occurs at around 700 Hz.

4. CONCLUSIONS

The present work uses the Newtonian approach-based analytical model to study the fully coupled vibroacoustic behavior of strip mass-loaded membranes which has not been attempted before. Results show that circular membranes with added strip mass are effective noise attenuators at the higher side of the low-frequency range. This finding will help design mass-loaded membranes for applications that require transmission peak/dip at higher frequencies within the low-frequency domain. The effect of multiple strip masses on the sound transmission characteristics of the membrane is a relevant future area of work.

REFERENCES

1. Christopher HM Jenkins and Umesh A Korde. Membrane vibration experiments: An historical review and recent results. *Journal of Sound and Vibration*, 295(3-5):602–613, 2006.
2. Yu Jia, Sijun Du, and Ashwin A Seshia. Micromachined cantilevers-on-membrane topology for broadband vibration energy harvesting. *Journal of Micromechanics and Microengineering*, 26(12):124007, 2016.
3. Felix Langfeldt, Wolfgang Gleine, and Otto von Estorff. Analytical model for low-frequency transmission loss calculation of membranes loaded with arbitrarily shaped masses. *Journal of Sound and Vibration*, 349:315–329, 2015.
4. R Pezone, G Baglioni, C van Ruiten, S Anzinger, HS Wasisto, Pasqualina M Sarro, PG Steeneken, and S Vollebregt. Effect of air-loading on the performance limits of graphene microphones. *Applied Physics Letters*, 124(12), 2024.
5. Hirsh Cohen and George Handelman. On the vibration of a circular membrane with added mass. *The Journal of the Acoustical Society of America*, 29(2):229–233, 1957.
6. CY Wang. Vibration of an annular membrane attached to a free, rigid core. *Journal of sound and vibration*, 260(4):776–782, 2003.
7. Kosuke Nagaya and Krzystof Poltorak. Method for solving eigenvalue problems of the helmholtz equation with a circular outer and a number of eccentric circular inner boundaries.

The Journal of the Acoustical Society of America, 85(2):576–581, 1989.

8. Kosuke Nagaya and Toshizumi Yamaguchi. Method for solving eigenvalue problems of the helmholtz equation with an arbitrarily shaped outer boundary and a number of eccentric inner boundaries of arbitrary shape. *The Journal of the Acoustical Society of America*, 90(4):2146–2153, 1991.
9. K Nagaya. Dynamics of viscoelastic plate with curved boundaries of arbitrary shape. *Journal of Applied Mechanics*, 1978.
10. Yangyang Chen, Guoliang Huang, Xiaoming Zhou, Gengkai Hu, and Chin-Teh Sun. Analytical coupled vibroacoustic modeling of membrane-type acoustic metamaterials: Membrane model. *The Journal of the Acoustical Society of America*, 136(3):969–979, 2014.
11. R Kirby and JB Lawrie. A point collocation approach to modelling large dissipative silencers. *Journal of sound and vibration*, 286(1-2):313–339, 2005.